

OBSERVATION OF PARTICLE ACCELERATION IN THE SOLAR CORONA WITH NEUTRON MONITORS AND RADIO INSTRUMENTS

K.-L. Klein¹

Abstract. In the attempt to identify regions and mechanisms of relativistic proton acceleration at the Sun, we compare the arrival of the first particles at Earth, measured by neutron monitors, with radio signatures of electron acceleration in the corona. The first proton arrival is often, but not always, delayed with respect to the early radio signatures at the Sun. But the release at the Sun always occurs at times when the radio emission is ongoing. This is in line with earlier studies of individual events, which made us conclude that relativistic protons are accelerated in flare-like processes related to magnetic reconnection or turbulence in the wake of a coronal mass ejection, rather than at the shocks driven by the ejected magnetic structures.

Keywords: Sun: particle emission, Sun: radio radiation, Sun: flares, Sun: coronal mass ejections (CMEs)

1 Introduction

The solar corona, structured by magnetic fields that emanate from the convection zone, accelerates episodically particles from suprathermal to sometimes relativistic energies. Energetic electrons can be probed in the solar atmosphere through their hard X-ray and radio emission, and ions through gamma-rays (see review by Vilmer and Musset, these proceedings). Due to its proximity, the Sun has the unique advantage that one can also probe directly energetic particle populations, provided they escape into the interplanetary space.

Spacecraft usually measure electrons up to MeV energies, and protons and ions up to about 100 MeV. Ground-based measurements of secondary particles generated by solar protons and ions in the Earth's atmosphere demonstrate that on occasion the Sun accelerates nuclei to GeV energies. The rarity of the events (one/year on average seen since 1942, but only three between 2006 and 2019) and the downward-curved shape of the energy spectra (Tylka & Dietrich 2009) show that the highest energies are in the GeV to a few tens-of-GeV range. While three such events were also detected in space by the PAMELA mission (Bruno et al. 2018), 72 have been seen by ground-based detectors, mostly detectors of secondary neutrons. These detectors are called neutron monitors. Particle events detected on the Earth are called ground-level events (GLEs).

Theory and modelling show that relativistic particles can in principle be accelerated in two different environments in the solar corona: in reconnecting current sheets (e.g., Heerikhuisen et al. 2002) and at large-scale shock waves (e.g., Afanasiev et al. 2018) driven by coronal mass ejections (CMEs). Since both processes occur in the eruptive events at the Sun that accompany GLEs, observational criteria are needed to identify which is most plausible. A key observable is the start time of a GLE, i.e. the time of detection of the first relativistic protons at the Earth, with respect to the timing of the particle acceleration in the solar corona. In the present report we compare the start time of relatively strong GLEs with the time evolution of electron acceleration in the corona, as traced by the radio emission.

2 Onset timing of relativistic solar particle events

Gopalswamy et al. (2012) measured the onset of 16 GLEs between 1997 and 2006, and concluded that it is later than expected if the first relativistic protons were accelerated together with the electrons in the associated flare traced by the rise of the soft X-ray emission. They ascribed the delay to the time needed by a CME to form a shock wave in the corona, and concluded that the accelerator of the relativistic protons was the shock,

¹ LESIA, Observatoire de Paris, Université PSL, CNRS, Sorbonne Université, Université Paris, 92190 Meudon, France

Table 1. Onset times and onset-time delays of GLEs.

Date	Duration		GLE start	Delay [min] (GLE-m- λ)	GLE start (Gopalswamy et al.)
	cm- λ	m- λ			
1997 Nov 06 OULU	11:52-12:10	11:52-14:00	12:08 (11:46,12:28)	16 (-6, 36)	12:10
2000 Jul 14 SOPO	10:10 (HXR)	10:16-10:40	10:34 (10:34,10:35)	18 (18, 19)	10:30
2001 Apr 15 SOPO	13:45-15:20	13:47-14:50	13:58 (13:58, 13:58)	11 (11, 11)	14:00
2003 Oct 28 MCMU	11:01-12:15	11:03-12:05	11:13 (11:10, 11:16)	10 (7, 13)	11:20
2003 Oct 29 SOPO	20:38-21:30	20:38-> 22 : 00	21:01 (21:00, 21:02)	23 (22, 24)	21:05
2005 Jan 20 TERA	06:38-08:00	06:44-07:50	06:49 (06:49, 06:49)	5 (5, 5)	06:50
2006 Dec 13 OULU	02:22-04:45	02:24-04:45	02:50 (02:49, 02:51)	26 (25, 27)	02:45
2017 Sep 10 FSMT	15:52-16:50	15:50-16:40	16:02 (15:57-16:06)	12 (7, 16)	-

rather than the reconnection processes in the lower corona. This conclusion was contradicted by the timing of the strongest GLE observed during the space age, on 2005 Jan 20 (Masson et al. 2009; Klein et al. 2014, and references therein). Those studies found that the onset of the GLE, which was particularly well-identified due to its fast rise, was consistent with acceleration since the early signatures of the associated flare at radio and hard X-ray wavelengths, as well as gamma-rays from pion-decay photons, which are due to protons or ions with energies comparable to those detected by neutron monitors. So there seems to be a contradiction between conclusions drawn from a sample of GLEs, and conclusions based on a detailed timing analysis of the best-observed event.

2.1 Determination of GLE onset

To explore this apparent contradiction, we conduct a new timing analysis of GLEs observed since 1997, with the exception of very weak events detected only marginally by neutron monitors. Neutron monitor data were provided by the neutron monitor data base NMDB (www.nmdb.eu) hosted at the University of Kiel. The start times were determined for the first responding neutron monitor, which detects particles that propagate along the heliospheric magnetic field. The usual estimate of the start time is the instant when the count rate exceeds the pre-event level. This is overestimated, since the previously existing signal is buried in the detector noise. In the present study start times were determined through a linear fit to the early rise of the logarithm of the count rate (i.e. it is supposed that the early rise is exponential). The start time given in col. 4 of Table 1 is the time when the straight line fit intersects the pre-event background. The values within parentheses give the times when the line intersects the pre-event background plus and minus three times the standard deviation. Column 5 is the delay with respect to the start of the m- λ emission. Column 6 gives the start times of Gopalswamy et al. (2012). These authors considered the onset as the time when the signal exceeded the background by at least 2%. The two determinations of the onset are consistent to within a few minutes. The start time determination is therefore not the reason for the conflicting conclusions.

2.2 Comparison with the timing of radio emission

Columns 2 and 3 of Table 1 give the onset and approximate end of the radio emission at centimetre and metre-wavelengths, inferred from whole Sun flux densities observed by the RSTN network of the US Air Force*. Delays of a few minutes are observed, with the m- λ emission lagging behind the cm- λ burst. Since higher frequencies correspond to lower coronal heights, this may show a confinement of the first accelerated electrons in the lower corona. The delays of the GLE start with respect to the start of the m- λ emission are listed in col. 5. A few GLEs start within a few minutes of the coronal signatures of electron acceleration. Since the travel time of protons of 450 MeV, which is the lower limit of the energy spectrum detectable by neutron monitors, and which travel at a speed of $0.75c$, is about 13 min (i.e. light travel time + 5 min), these delays may be consistent with acceleration of the first protons of the GLE in the very early phase of energy release in the corona, which points to the parent flare and the associated magnetic reconnection and turbulence. Among them is the 2005 Jan 20 GLE, for which Masson et al. (2009) demonstrated the relationship in detail. The 1997 Nov 06 GLE has a very uncertain start, due to a long shallow rise. Three GLEs have more substantial delays (18-26 min).

*Data provided by the National Centers for Environmental Information (NOAA) <https://www.ngdc.noaa.gov/stp/space-weather/solar-data/solar-features/solar-radio/rstn-1-second/>

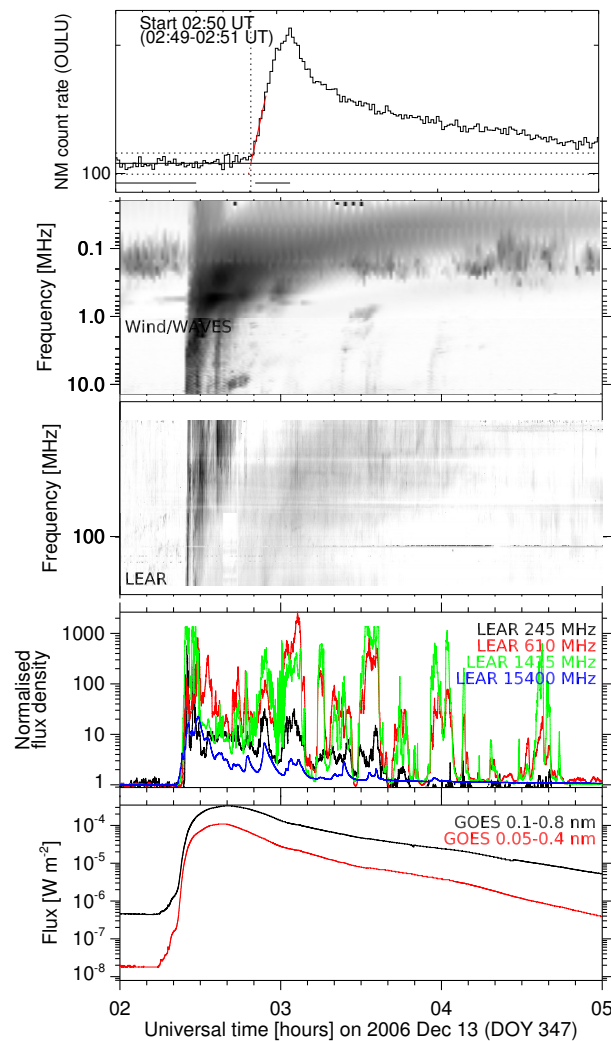


Fig. 1. Time history of soft X-ray and radio emission associated with the relativistic solar proton event on 2006 Dec 13. From bottom to top: thermal soft X-ray emission, cm-m- λ emission at fixed frequencies, dynamic spectra at long metre waves (180-30 MHz; dark shading shows bright emission) and decametre-to-kilometre waves (14 MHz-20 kHz). The ordering of the radio waves from high to low frequencies roughly corresponds to progression from the chromosphere (15400 MHz) through the high corona (10 solar radii at 1 MHz) to 1 AU. The top panel shows the count rate time history of the Oulu neutron monitor and the fit (red line) used to derive the onset time.

2.3 An illustration: the GLE on 2006 Dec 13

While the GLEs may start up to 20-30 minutes after the accompanying radio emission, all radio bursts have an extended duration. The long duration indicates the time-extended acceleration of electrons in the corona. Figure 1 displays the soft X-ray (bottom) and radio emission during the event with the longest onset delay. The second panel from the bottom shows the whole-Sun emission at selected frequencies. Microwave emission (15400 MHz) is gyro-synchrotron radiation of near-relativistic electrons (hundreds of keV to some MeV), while m- λ emission is generally ascribed to plasma instabilities. In this case the radio emission in the cm-m-band shows correlated strong variability, independent of the emission process. This suggests that electrons are accelerated in a 2-3 hours-lasting series of impulsive events. The third panel from bottom shows the dynamic spectrum at long metre waves. The initial bright bursts (“type III” bursts) are produced by electron beams that travel outward through the corona. Their spectrum extends into the decametre-to-kilometre waveband as shown in the Wind/WAVES (Bougeret et al. 1995) observations in the second panel from top. The m- λ type III bursts

are followed by a fainter broadband continuum (“type IV” burst) from a confined electron population. The acceleration is related to a different process, probably occurring in a current sheet behind the rising CME. The downward drift of the high-frequency border shows that the radio source takes part in the rise. The start of the continuum and of the GLE (near 02:50 UT) are close in time. At the time of the continuum the WAVES spectrum shows faint traces of short bursts similar to the type III bursts. The time coincidence suggests they are tracers of electrons escaping from the type IV radio source in the middle corona to interplanetary space.

Another feature of the WAVES spectrum are two bright packets of narrow-band bursts (near 02:40 around 10 MHz, near 03:30 at a few hundreds of kHz). They are part of a burst ascribed to electrons accelerated at the shock wave driven by the corona. The gradual outward progression of the shock explains the gradual shift of the emission to lower frequencies (“type II” burst). The emission demonstrates that at the time of the long-lasting electron acceleration shown at cm-m- λ a shock wave has been formed by the outward-travelling CME.

3 Discussion

The arrival of relativistic protons and ions accelerated in solar eruptive events is often, but not always, delayed with respect to the earliest signatures of particle acceleration at the Sun, especially of electron acceleration as traced by hard X-ray and radio emissions. This delay, which is well known in the literature, has been often interpreted as the time that a CME needs to form a shock wave, which subsequently accelerates the particles detected in space. The present study demonstrates, however, that this is not the only possible interpretation. For at the time when the particles are released near the Sun electron acceleration is ongoing in the corona. The extended emission from microwaves to metre waves shows indeed that the acceleration occurs within one solar radius above the photosphere. The observed GLE start could therefore be consistent with particle acceleration in the low corona, sometimes starting with the first flare signatures (as on 2005 Jan 20, Masson et al. 2009), more often during later phases of the eruptive event, after the liftoff of the CME. The late radio emission, and hence by inference the relativistic proton acceleration, would occur in the wake of the CME where the stressed coronal magnetic field relaxes. It does so through magnetic reconnection in current sheets below the magnetic flux rope that forms the core of the CME, or in the turbulence generated during the CME liftoff. The accelerated particles could escape to the interplanetary space via reconnection of the magnetic field in the CME with ambient open field lines, which likely proceeds as the CME travels outwards (Masson et al. 2013).

The radio emission in Figure 1 shows also that a CME-driven shock wave exists at the time of the late relativistic proton acceleration. This makes the interpretation of a single event ambiguous. In the present author’s view the fact that in detailed event studies the onset - and in the 2005 Jan 20 event also a second late release - occurs with distinct episodes of electron acceleration in the solar corona (Klein et al. 1999; Masson et al. 2009; Klein et al. 2014) rather supports the view that the particles are accelerated behind the CME, not at its shock wave.

The *Parker Solar Probe* (NASA) and *Solar Orbiter* (ESA/NASA) space missions will provide energetic particle measurements much closer to the Sun than 1 AU. The particle signatures will then be much less distorted by the turbulent heliospheric magnetic field than in traditional measurements. This should allow better-documented conclusions on the acceleration region. The response may depend on the particle energy. Since in situ measurements are limited to about 100 MeV, neutron monitors on Earth will remain state-of-the-art to investigate acceleration to the highest energies that the Sun may produce.

References

- Afanasiev, A., Vainio, R., Rouillard, A. P., et al. 2018, *A&A*, 614, A4
 Bougeret, J.-L., Kaiser, M. L., Kellogg, P. J., et al. 1995, *Space Sci. Rev.*, 71, 231
 Bruno, A., Bazilevskaya, G. A., Boezio, M., et al. 2018, *ApJ*, 862, 97
 Gopalswamy, N., Xie, H., Yashiro, S., et al. 2012, *Space Sci. Rev.*, 171, 23
 Heerikhuisen, J., Litvinenko, Y. E., & Craig, I. J. D. 2002, *ApJ*, 566, 512
 Klein, K.-L., Chupp, E. L., Trottet, G., et al. 1999, *A&A*, 348, 271
 Klein, K.-L., Masson, S., Bouratzis, C., et al. 2014, *A&A*, 572, A4
 Masson, S., Antiochos, S. K., & DeVore, C. R. 2013, *ApJ*, 771, 82
 Masson, S., Klein, K.-L., Bütikofer, R., et al. 2009, *Sol. Phys.*, 257, 305
 Tylka, A. & Dietrich, W. 2009, in 31st International Cosmic Ray Conference, ed. M. Giller & et al. (<http://icrc2009.uni.lodz.pl/proc/pdf/icrc0273.pdf>)